

Simulating tumor growth in confined heterogeneous environments

Jana L Gevertz¹, George T Gillies^{2,3,4} and Salvatore Torquato^{1,5,6,7,8}

¹ Program in Applied and Computational Mathematics, Princeton University, Princeton, NJ 08544, USA

² Department of Physics, University of Virginia, Charlottesville, VA 22904, USA

³ Department of Biomedical Engineering, University of Virginia, Charlottesville, VA 22908, USA

⁴ Department of Neurosurgery, Virginia Commonwealth University, Richmond, VA 23298, USA

⁵ Department of Chemistry, Princeton University, Princeton, NJ 08544, USA

⁶ Princeton Institute for the Science and Technology of Materials, Princeton University, Princeton, NJ 08544, USA

⁷ Princeton Center for Theoretical Science, Princeton University, Princeton, NJ 08544, USA

E-mail: torquato@princeton.edu

Received 6 May 2008


Accepted for publication 12 August 2008

Published 29 September 2008

Online at stacks.iop.org/PhysBio/5/036010

Abstract

The holy grail of computational tumor modeling is to develop a simulation tool that can be utilized in the clinic to predict neoplastic progression and propose individualized optimal treatment strategies. In order to develop such a predictive model, one must account for many of the complex processes involved in tumor growth. One interaction that has not been incorporated into computational models of neoplastic progression is the impact that organ-imposed physical confinement and heterogeneity have on tumor growth. For this reason, we have taken a cellular automaton algorithm that was originally designed to simulate spherically symmetric tumor growth and generalized the algorithm to incorporate the effects of tissue shape and structure. We show that models that do not account for organ/tissue geometry and topology lead to false conclusions about tumor spread, shape and size. The impact that confinement has on tumor growth is more pronounced when a neoplasm is growing close to, versus far from, the confining boundary. Thus, any clinical simulation tool of cancer progression must not only consider the shape and structure of the organ in which a tumor is growing, but must also consider the location of the tumor within the organ if it is to accurately predict neoplastic growth dynamics.

 This article features online multimedia enhancements

Abbreviations list

CA	cellular automaton
ISF	interstitial fluid
RSA	random sequential addition

1. Introduction

Computational modeling of tumor growth has been an active area of research for the last several decades. An extremely

diverse number of mechanisms have been explored via such models, and a multitude of computational/mathematical techniques have been employed. While there is a large amount of diversity in existing computational models, all models have the common aim of predicting certain features of tumor growth in the hope of finding new ways to either control, stop or reverse neoplastic progression. Given a model which yields reproducible and accurate predictions, the effects of different genetic, epigenetic and environmental changes, as well as the impact of therapeutically targeting different aspects of the tumor, can be probed via computer simulations. This allows modeling to guide and augment experimentation,

⁸ Author to whom any correspondence should be addressed.

as new biological/basic research questions can be explored *in silico* before performing costly experiments.

While computer models of tumor growth have, in some instances, proven successful at driving experimentation, another important role for tumor modeling can be found in the clinic. Perhaps the most important goal of computational tumor modeling is to reliably predict cancer progression with only a limited amount of data on a patient's tumor type and location (e.g., genetic data from biopsy samples and tumor morphologies from magnetic resonance or computed tomography imaging studies). Such a model would not only allow an oncologist to predict tumor progression, but can also help them to develop a more individualized treatment strategy for each cancer patient.

Given the enormous number of factors that drive tumor growth and determine treatment response, one would expect that such a model must incorporate the many complexities of tumor growth. Much progress has been made in incorporating a number of genetic, cellular and tissue properties, as well as some same-scale and multi-scale interaction loops, into tumor growth models. Although a comprehensive exploration of all such models is beyond the scope of this text, one point that should be noted is that, to our knowledge, no models of tumor growth account for the structure and composition of the organ in which the tumor grows, or the location of the tumor within the organ. Hence, in this paper we propose an algorithm that considers the impact that physical confinement and organ heterogeneity have on tumor shape, size and spread.

Before discussing our model, it is useful to briefly explore the types of features that computational tumor models have been able to incorporate. Several models have explored the impact that different sequences of genetic mutations have on tumor emergence and survival [1, 2]. Models that incorporate the impact of genetic mutations tend to be focused inward on changes that occur within the cell. Other classes of models have also looked outward, for example considering the competition for space and resources that occurs between normal and cancerous cells [3, 4]. Another type of competition that has been modeled is that between the immune system and the neoplastic mass [5, 6]. The immune system is especially important to consider when simulating the response of tumors to different treatment strategies, which will be an essential aspect of any model with clinical applications. Although thus far we have only discussed competitive feedback, the tumor can also alter the host in ways that are beneficial for its development, for example by altering the blood supply to fit the needs of the tumor [7, 8].

From a strictly mechanical perspective, the presence of a solid mass growing in healthy tissue produces solid stress. Models (see [9–11] for a noncomprehensive list) have also been developed to look at this form of mechanical feedback in which the tumor deforms the surrounding tissue due to the stress it imposes on the environment, and the environment in turn alters tumor growth dynamics. In this set of models, tumor growth inhibition depends on the stiffness of the surrounding environment. In an *in vitro* setting, this corresponds to the stiffness of the agarose gel, and *in vivo* this corresponds to the stiffness of the extracellular matrix environment [12].

Interestingly, we note that agarose gels also serve another function as *in vitro* models of tissues: test beds for evaluating the convection-enhanced flow of antitumoral agents delivered interstitially within the brain via positive pressure infusion [13]. While these mechanical models are useful in studying the response of a tumor to solid stress, they do not address the complications that arise when tumors grow in physically confined and heterogeneous spaces such as the brain or near an organ boundary.

Biomechanical analysis methods have also been utilized in yet another class of tumor growth models in order to address the somewhat counterintuitive point that the surgical debulking of brain tumors (i.e., creating space within the brain), which is an absolute clinical necessity, can actually lead to induced regrowth within the peritumoral region, as proposed in [14]. Finally, we note that there has also been a movement toward modeling the cellular-scale phenomena that take place in the peritumoral region, and that these efforts represent touch points between mechanistic statistical approaches to understanding tumor growth and those that are centered largely on pathological observations. For the case of primary malignant brain tumors, these include studies of the nanodynamics of invadopodial extension from glioma cells as measured by atomic force microscopy [15], chemotactic signaling as a possible means for initiating tumor growth by producing targeted movement of one glioma cell toward another [16], and glioma cell invasion as driven by the flow of the interstitial fluid [17]. In this paper, we seek to extend the analytical/computational understanding of tumor growth by incorporating geometric confinement and heterogeneity issues in ways that will ultimately impact the clinical utility of such biophysical models across the spectrum of approaches.

The effects of physical confinement on tumor growth have been studied experimentally. In pioneering work done by Helmlinger *et al* [12], LS174T human colon adenocarcinoma cells were grown in cylindrical glass tubes with a radius that is much smaller than the length of the tube. They found that cell aggregates in 0.7% gel placed in a capillary tube grew to take on an ellipsoidal shape, driven by the geometry of the capillary tube. However, the same cells grown outside a capillary tube developed into a spheroid-shaped tumor. This experiment clearly highlights that geometric confinement alters the shape and growth dynamics of a developing tumor [12]. However, to our knowledge, no existing model of tumor growth accounts for geometric confinement effects on the size and shape of a growing tumor.

In keeping with the goal of developing a clinically relevant cancer simulation tool that accurately predicts *in vivo* tumor growth dynamics, shape and spread throughout an organ, computational models must consider the location of a tumor within the organ, and the physical constraints placed on growth by that organ. In this paper, we modify an existing computational model of tumor growth [18] to incorporate the effects of environmental confinement and heterogeneity on neoplastic progression. We show that failure to account for organ geometry and topology leads to inaccurate predictions about the size, shape and spread of the tumor after sufficiently large times.

2. Methods

In order to simulate tumor growth in confined heterogeneous environments, we have adapted a cellular automaton (CA) model developed by Kansal *et al* [18]. Using this model, it was shown that three-dimensional tumor growth and composition can be realistically predicted by four microscopic parameters that account for the nutritional needs of the tumor, cell-doubling time and an imposed spherical symmetry term [18]. This model has been used as the basis for a second study, in which a distinct subpopulation was introduced into a homogeneous tumor. It was shown that the emergence and survival of one subpopulation can drastically alter tumor growth dynamics, suggesting that prognosis based on the assumption of a monoclonal tumor can be markedly inaccurate [19]. The original CA model has also been applied to study the effectiveness of chemotherapy applied after surgery. It was shown that patient prognosis is severely compromised when chemotherapy-resistant cells are not localized in the neoplasm [20]. In these versions of the model, oxygen and nutrient levels were implicitly determined by the distance of a cell from the tumor's edge and center, as well as by the four microscopic parameters in the algorithm. This simplification was made in an attempt to develop a minimalistic model of tumor growth. In order to incorporate a higher level of biological realism, we have also modified the CA model to study the feedback that occurs between the growing tumor and the evolving host blood supply [8]. This way, the state of each cancer cell is determined by the blood supply and oxygen levels.

In all four of these studies, the effects of mechanical confinement were limited to one parameter R_{\max} , which imposes a maximum radius on a spherically symmetric tumor. In order to generalize the CA model so that it can be applied to tumors growing in organs of any shape with nonhomogeneous tissue structure in an arbitrary Euclidean space dimension d , it is necessary to remove all radially symmetric assumptions from the evolution rules. We have intentionally chosen to generalize the original CA model instead of jumping to incorporate the effects of physical confinement and environmental heterogeneity into a more advanced model, such as the vascular growth model. This is because we want to verify that these rules are viable in a *simplified* model of tumor growth before utilizing the rules in a more complex model. If the modified rules were not successful to grow simplified tumors, they would certainly fail if we tried to implement the rules in a model with a higher level of complexity. Further, taking this approach is similar to how we developed the vascular algorithm—we first developed a set of simple rules that qualitatively mimicked tumor growth, and at a later time we added the biological detail of the vasculature. Our goal is not to build up complexity until we can be assured that the individual pieces yield qualitatively realistic and relevant results. Finally, we have shown in [8] that vasculature incorporation does not qualitatively change the shape and size of a growing tumor, meaning we are not sacrificing much at an early stage by using the original CA model instead of the vascular growth algorithm.

In this section, we will discuss the changes that must be made to the original CA algorithm in order to account for

the effects that physical confinement and organ heterogeneity have on tumor growth. As we describe the new algorithm, we also explicitly state how the new algorithm is similar to, and differs from, the original CA model, thus presenting the steps involved in both algorithms simultaneously. In a future paper, we will tackle the problem of merging the confined and heterogeneous growth algorithm with the vascular algorithm.

The first step required to generalize the original CA algorithm is to define the 'growth-permitting region'; that is, the environment in which the tumor can grow. The tissue region is initialized by generating the automaton cells. In both algorithms, the fixed underlying lattice for our algorithm is the Delaunay triangulation, which is the dual lattice of the Voronoi tessellation [18, 21]. In order to develop the automaton cells (which can be thought of as representing a cluster of biological cells), a prescribed number of random points are generated using the process of random sequential addition (RSA) of hard circular discs [18, 21]. Points that fall too close to any other point are rejected, and all others are added to the system. Each cell in the final Voronoi lattice will contain exactly one of these accepted sites. The Voronoi cell is then defined by the region of space nearer to a particular site than any other site. In two dimensions, the RSA points are fed to a program based on the sweepline Voronoi algorithm developed by Fortune [22], and the result is a collection of polygons that fill the plane. In three dimensions, the points are fed to an algorithm developed by Donev *et al* [23], and the result is a collection of polyhedra that fill space. Once the automaton cells have been created, the new algorithm requires that cells must be divided into one of the two regimes: automaton cells within the growth-permitting environment and automaton cells within the growth-prohibiting environment. The boundary between the two cell types can be arbitrarily chosen by the user, or can be chosen to match the structure of a particular organ. In order to illustrate the versatility of the algorithm, we will consider tumor growth in four distinct regions: an ellipse, a random two-dimensional asymmetric environment, a two-dimensional representation of the cranium and a three-dimensional ellipsoid.

We can now consider the algorithm that is used to study tumor progression in confined heterogeneous regions. After performing the first step of determining the automaton cells and denoting each cell as either growth-permitting or growth-prohibiting, a tumor is introduced into the tissue by designating any one or more of the growth-permitting automaton cells as a proliferative cancer cell. Time is then discretized into units that represent one real day. At each time step

- Each cell is checked for type: nonmalignant, proliferative, quiescent or necrotic. Proliferative cells are actively dividing cancer cells, quiescent cancer cells are those that are alive, but do not have enough oxygen and nutrients to support cellular division and necrotic cells are dead cancer cells. This step occurs in both the original and modified algorithms.
- In both versions of the algorithm, nonmalignant cells and tumorous necrotic cells are inert. While nonmalignant cell division occurs in some organs, a hallmark of neoplastic growth is that tumor cells replicate significantly faster than

the corresponding normal cells. Hence, we work under the simplifying assumption that nonmalignant division rates are so small compared to neoplastic division rates that they become relatively unimportant in the time scales we are considering. In those cases where this does not hold, nonmalignant cellular division would have to be incorporated into the model.

- Quiescent cells more than a certain distance δ_n from the tumor's edge are turned necrotic. The tumor's edge, which is assumed to be the source of oxygen and nutrients, consists of all healthy cells that border the neoplasm. In the original algorithm, δ_n depended on a nutritional parameter a and the current radius of the tumor. Since the algorithm is now being adapted to consider asymmetric tumor growth, we instead define the following critical distance for quiescent cells to turn necrotic:

$$\delta_n = aL_t^{(d-1)/d},$$

where d is the dimension of the tissue and tumor in the model and L_t is the distance between the geometric center of the tumor, given by (x_1^c, \dots, x_d^c) , and the tumor edge cell that is closest to the quiescent cell under consideration. The center coordinates x_i^c for all $i \leq d$ are given by

$$x_i^c = \frac{x_i^1 + \dots + x_i^k}{k},$$

where k is the number of automaton cells contained within the tumor.

- Each proliferative cell will attempt to divide with probability p_{div} into the space of a growth-permitting nonmalignant cell. If division does occur, the daughter cell 'takes the place of' the closest nonmalignant cell via an intercellular mechanical stress algorithm [18] that essentially forces the nonmalignant cell being replaced into the surrounding region of indistinguishable nonmalignant cells. In the original algorithm, the probability of division depended on the distance of the dividing cell from the tumor center r and the maximum tumor radius R_{max} . Since we generally no longer expect tumor growth to be radially symmetric, we replace R_{max} with a new parameter L_{max} , which is defined to be the distance between the closest nonmalignant boundary cell in the direction of tumor growth and the tumor's geometric center. We define the probability a proliferative cell divides to be

$$p_{\text{div}} = \begin{cases} p_0(1 - r/L_{\text{max}}) & \text{if any nonmalignant cell} \\ & \text{within the pre-defined} \\ & \text{growth distance is in the} \\ & \text{growth-permitting} \\ & \text{environment} \\ 0 & \text{if no nonmalignant cell within} \\ & \text{the pre-defined growth} \\ & \text{distance is in the growth-} \\ & \text{permitting environment,} \end{cases}$$

where p_0 is the base probability of division and the predefined growth distance δ_p is described in the following bullet point. It is worth noting that in this

piecewise definition of p_{div} , the type of all healthy cells (that is, growth-permitting or prohibiting) within a fixed distance of the proliferative cell under consideration determines whether or not the cell has a nonzero probability of division. Importantly, we do not have to worry about a negative probability of division because both cells that determine the values of r and L_{max} are at the same angle from the tumor center. Since the cell determining r is within the boundaries of the growth-permitting region, and since the cell determining L_{max} defines the boundary, we are guaranteed that $r \leq L_{\text{max}}$ and that the probability of division is always non-negative.

- A proliferative cell turns quiescent if there is no space available for the placement of a daughter cell within a distance δ_p from the proliferative cell. In the original algorithm, this critical distance depended on both a nutritional parameter b and the tumor radius. To remove the dependence on the tumor radius from the algorithm, we define the following critical distance for a proliferative cell to turn quiescent:

$$\delta_p = bL_t^{(d-1)/d},$$

where again d is the spatial dimension and, in this case, L_t is the distance between the geometric tumor center and the tumor edge cell that is closest to the proliferative cell under consideration.

- In both versions of the model, the geometric center of the tumor must be recalculated after each iteration of the algorithm.

We note that despite all the changes made to the original automaton rules, the modified algorithm behaves just as the original algorithm in the special case of a radially symmetric environment.

In the current investigation, both the original set of automaton evolution rules and the modified rules are applied to tumors growing in the aforementioned confined regions. This allows us to evaluate the impact that the radially symmetric assumption has on predicting tumor shape, size and spread throughout an organ.

3. Results and discussion

Tumor growth has been simulated in a variety of confined environments. The environment considered can either have a vascular boundary, meaning a growing tumor can receive oxygen from the growth-permitting region, or an avascular boundary, in which the growth-prohibiting region cannot supply the growing tumor with oxygen. In the visualizations of the tumor that follow, we use the following convention: nonmalignant cells in the growth-permitting environment are white, necrotic tumor cells are black, quiescent tumor cells are yellow and proliferative tumor cells are blue. Nonmalignant cells in the growth-prohibiting region that are separated from the growth-permitting region by a vascular boundary are shown in green, whereas those separated by an avascular

boundary are shown in grey. In the simulations described below, the following parameter values are utilized:

$$p_0 = 0.192, \quad a = 0.15 \text{ units}^{1/2} \text{ (in 2D),}$$

$$a = 0.12 \text{ units}^{1/3} \text{ (in 3D),} \quad b = 0.08 \text{ units}^{1/d},$$

where the value of p_0 chosen corresponds to a cell-doubling time of approximately four days. We have pre-selected these parameter sets because, when using the original CA model, they reproduce a test case from the medical literature (see [18] for the test case). Further, when we run the old algorithm for comparisons sake, we take the maximum tumor radius to be $R_{\max} = 0.4$ units. We have intentionally used an arbitrary unit of length in our model instead of defining a precise one. Both the size of the cells in the organ being considered and the resolution of the algorithm (that is, how many biological cells are found within one automaton cell) need to be considered to convert the arbitrary units used in the model to physical units. For example, if we want to consider glioma growth in the brain, the average glial cell has a diameter of $40 \mu\text{m}$ [24]. If we assume that there is a one-to-one correspondence between a glial cell and an automaton cell, then the average diameter of an automaton cell (which is 0.00257 units in our 2D simulations) is equivalent to $40 \mu\text{m}$, and $1 \text{ unit} \approx 15.5 \text{ mm}$. We can increase the size of the region by incorporating more than one biological cell inside an automaton cell.

We begin by considering tumor growth in confined two-dimensional regions with vascular boundaries. The first growth-permitting environment we consider is that of an ellipse with a major to minor axes ratio of 1.5. If tumor growth initiates at the center of the ellipse, we find that at early times, the neoplasm is radially symmetric, just as would be predicted using the original automaton rules (figures 1(ai) and (aiii)). However, as time progresses and the tumor begins to encroach upon the boundary of the growth-permitting region, the neoplasm transforms to take on the shape of the elliptical environment (figure 1(aii)). A comparison of the tumor's growth rate predicted by the original and modified algorithms reveals that only after a sufficiently long time does the elliptical shape of the growth-permitting region exert any effect on the area of the tumor. Nonetheless, after one year the shape of the growing tumor is dramatically affected, as the original algorithm predicts that the tumor would be a circle, whereas the modified algorithm predicts that the tumor is an ellipse with a major to minor axes ratio of 1.35.

We see that when the tumor initiates in the center of the growth-permitting region, the differences between the predictions of the original and the modified algorithms are not revealed until after over eight months of growth, as it takes this long for the tumor to 'sense' the boundary. It is then interesting to ask how the original and modified algorithms compare if the tumor initiates close to this boundary (figure 1(b)). In this case, we find that after only two months of tumor growth, the shape and growth dynamics predicted by the two algorithms begin to noticeably differ. Thus, the closer the growing tumor is to the boundary which is constraining its growth, the more important it is to account for the effects of this confinement.

It is important to note that these results are not dependent on the axisymmetric nature of the growth-permitting region.

To prove this point, we have also simulated tumor growth in a random asymmetric environment (figure 1(c)). As was observed with the elliptical environment, at small times the tumor is circular, just as predicted by the original algorithm. However, after about one year of growth using the new algorithm, the shape of the tumor is drastically altered from that of a circle due to the constraints imposed by the confining boundary. We conclude that in two dimensions, the algorithm can predict tumor growth in constrained environments in a manner far superior to what would be predicted from an algorithm that assumes radial symmetry.

The automaton rules easily generalize to three dimensions. In figure 2, a tumor developing in an ellipsoid-shaped environment with a major to minor axes ratio of 1.5 can be seen at both an early and a late stage of growth. Just as was observed in two dimensions, at early times the tumor does not 'sense' its boundary and grows in a radially symmetric fashion (figure 2(a)). After a sufficient amount of time has passed however, the tumor begins to encroach on the confining boundary, and the neoplasm begins to take the form of the growth-permitting region (figure 2(b)). This three-dimensional example can be compared to the experiment in which a tumor spheroid developing in a capillary tube grows to take on an ellipsoidal shape [12]. In our simulations, the modified algorithm accurately predicts that the tumor takes on an ellipsoidal shape as it grows in a region comparable in shape to that of a capillary tube. However, the original algorithm erroneously predicts that a tumor growing in a capillary tube will take on a spherical shape. In experiments, this shape is only observed when the tumor grows in a non-confined gel [12]. This highlights the importance of considering physical confinement effects in simulations of tumor growth.

Up to this point, we have only considered tumor growth in homogeneous regions confined by a vascular boundary. However, several organs contain vascular and avascular obstacles to growth and hence have a heterogeneous tissue structure. An example of this is the brain; tumors growing in the brain are confined by the cranium, but within the cranium, brain ventricles provide avascular obstacles to tumor growth (figure 3(a)). Keeping the shape of the cranium and the nature of the brain ventricles in mind, we have tested the proposed algorithm on an elliptic region with a vascular boundary (representing the cranium), and we have added two growth-prohibiting circular obstacles (representing the brain ventricles). We find that incorporating ventricles inside the growth-permitting region causes the predictions made from the original and modified algorithms to drastically differ. As can be seen in figure 3, the tumor must substantially change its geometry and topology at a relatively early point in time due to the presence of the ventricles inside the growth-permitting region. This highlights the importance of accounting for tissue heterogeneity in computational models of tumor growth.

The final phase of tumor development is the growth-limiting plateau in which the size of the tumor essentially remains unchanged with time. This phase usually corresponds to the tumor filling the available space or the tumor outgrowing its nutrient supply. A trend occurring in all of the simulations is

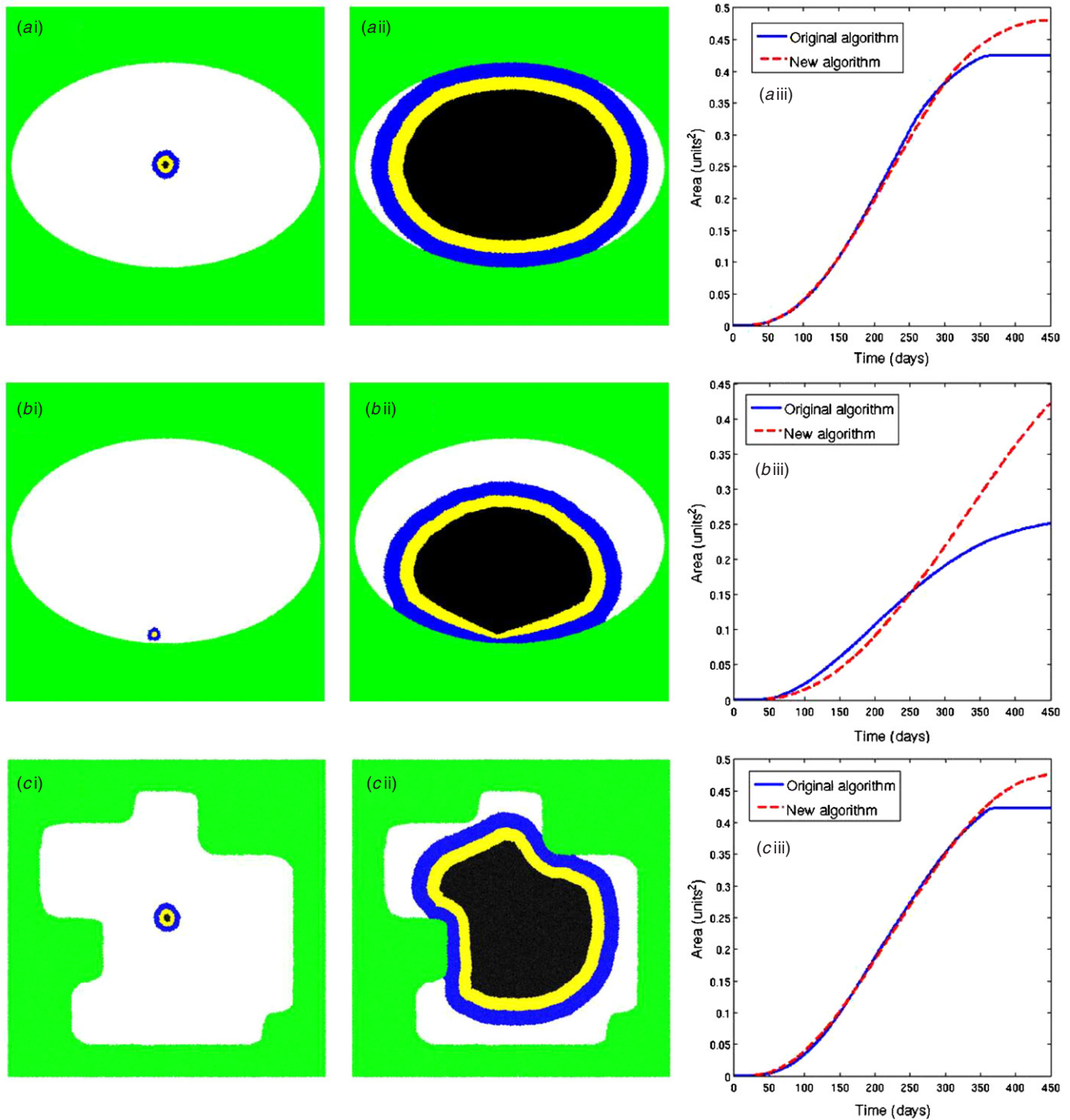


Figure 1. Tumor growth in different confined 2D homogeneous regions with vascular boundaries. (a) In an elliptic environment with the tumor initiating in the region center and shown after (i) 50 days and (ii) 350 days. (b) In an elliptic environment with the tumor initiating close to the region boundary and shown after (i) 50 days and (ii) 350 days. (c) In a random asymmetric environment with the tumor initiating in the region center and shown after (i) 50 days and (ii) 250 days. In each case (iii) contains growth curves that compare the tumor size as a function of time as predicted by the new algorithm (dashed red line) and the original algorithm (solid blue line).

that either the size of the tumor at the growth-limiting plateau, or the onset of this plateau, differs between the original and newly proposed algorithms. From a clinical perspective, this finding is very important. Our simulations have shown that if the tumor is identified early enough, the shape and size of the tumor may not bear the marks of the environment in which it grows. Yet, if we want to successfully predict the future time course of the tumor, the prognosis between the

two algorithms differ significantly. If we look at the confined homogeneous environments in figures 1(a) and (c), the growth-limiting plateau is achieved around the same time using the original and modified simulations, yet the ultimate size the tumor reaches at the plateau is larger when the algorithm accounts for environmental confinement. If we consider the elliptic environment with the tumor starting close to the boundary (figure 1(b)), not only can the tumor grow to a larger

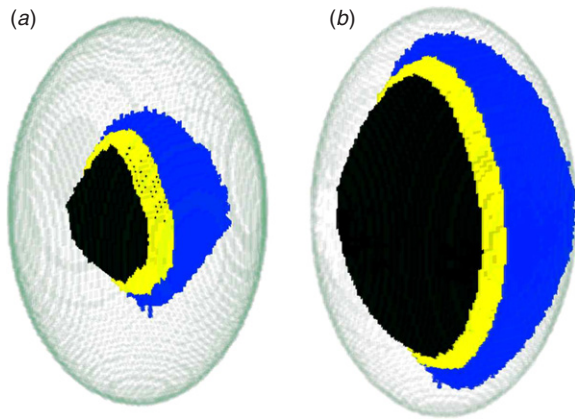


Figure 2. Three-dimensional tumor growth in a homogeneous ellipsoidal environment with a vascular boundary. Tumor growth initiates in the region center and is shown after (a) 50 days and (b) 225 days.

size when the newly proposed algorithm is used, the onset of the growth-limiting plateau occurs at a substantially later time than when the original automaton rules are applied. Thus,

depending on the region in which the tumor grows and the location of the tumor within the region, both the size of the tumor at the growth-limiting plateau phase and the time it takes to reach this phase differ between the original and new model. This further highlights the importance of including environmental confinement and heterogeneity in establishing the prognosis of a cancer patient. In previous work [19], it was similarly shown that the assumption of a homogeneous tumor can lead to errors in predicting both patient history and prognosis. This suggests that incorporating both tumor and environmental heterogeneity into one algorithm can further enhance the predictability of the model.

4. Conclusion and outlook

A computer simulation tool that can be utilized to predict neoplastic progression in the clinic must necessarily account for as many of the complex processes involved in tumor growth as possible. Treatment plans based on the use of such modeling and simulation processes will require rigorous validation studies, regulatory approvals and, then, eventual

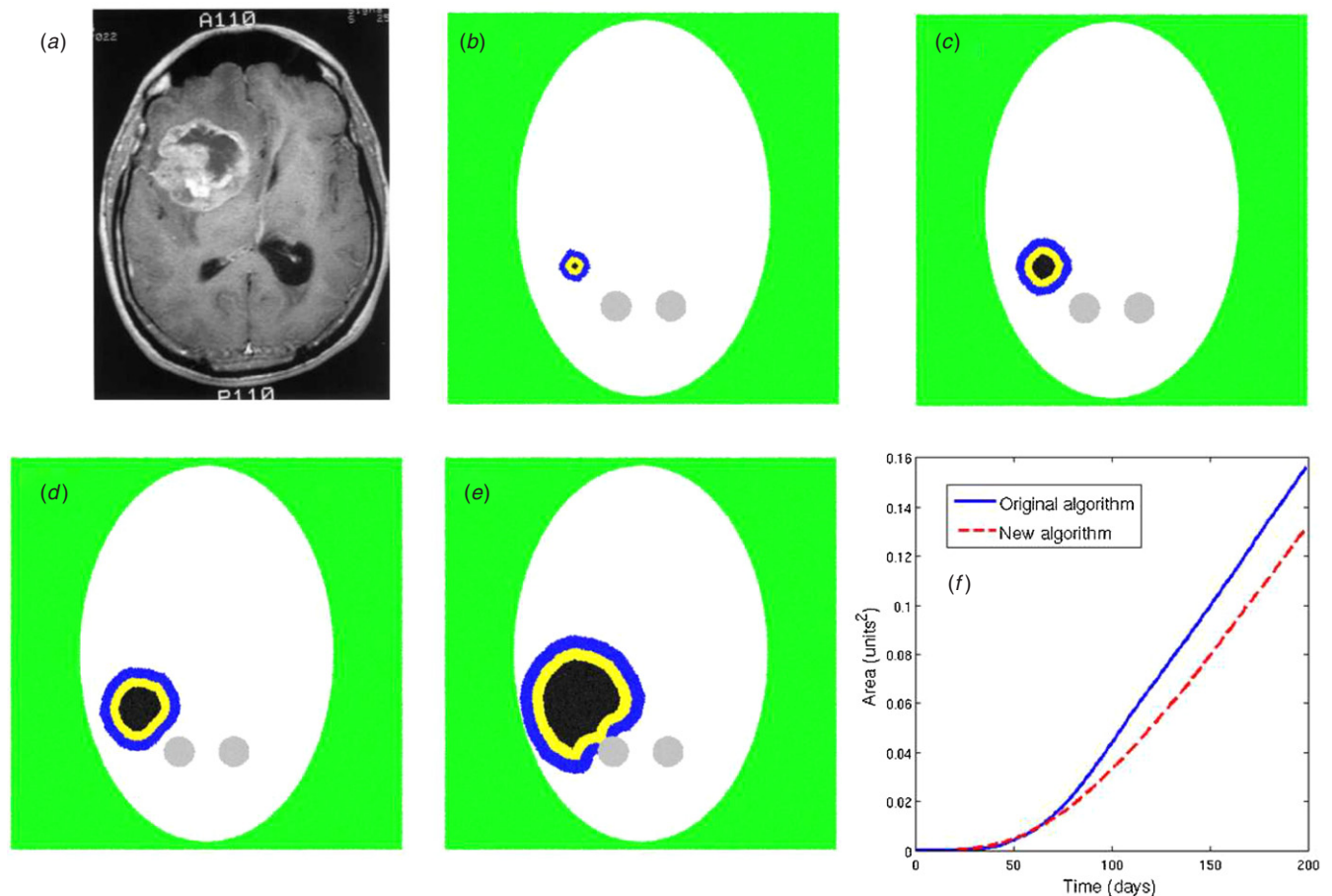


Figure 3. Tumor growth in a 2D representation of the brain. (a) T1-contrast-enhanced brain MRI-scan with a right frontal GBM tumor [18] suggests how to represent the brain macroenvironment. (Reprinted from [18], with permission from Elsevier, copyright (2000).) In our representation of this environment, the tumor is shown after (b) 50 days, (c) 75 days, (d) 100 days and (e) 125 days. The growth curves shown in (f) compare the tumor size as a function of time as predicted by the new algorithm (dashed red line) and the original algorithm (solid blue line).

M An AVI movie of this figure is available from stacks.iop.org/PhysBio/5/036010

integration into the armamentarium of oncological practice. Some examples of image-based treatment planning tools being developed within this spirit are intra-cranial infusion-therapy delivery systems. Early work in this area includes the original studies by Morrison *et al* [25] at the NIH and later, the *in vitro* and *in vivo* investigations by Chen *et al* [26] and Haar *et al* [27], among many such efforts by others (see [28, 29] for reviews). Sophisticated clinical trials were then carried out by Sampson *et al* [30], with approval and commissioning of the resulting software for use in the neurosurgical arena; see [31]. While most presently available treatment planning systems are able to optimize the potential efficacy of a therapy given the observed, existing anatomical and physiological state of the tumor, they are not generally designed to be comprehensive modeling tools that predict tumor growth patterns as well. Therefore, as the work in this area progresses toward such a broader goal, one interaction between the host and the growing tumor that will need to be included in computational models of tumor progression is the impact that the geometry and topology of a tissue region have on the shape and size of a developing neoplasm. For this reason, we have taken a cellular automaton algorithm that was originally designed to simulate spherically symmetric tumor growth and generalized the evolution rules to allow the tumor to grow in an arbitrary environment with either a homogeneous or heterogeneous tissue structure. We have tested both the original and modified algorithms in a variety of environments, and we have found that algorithms that ignore the impact of tissue structure inaccurately predict the volumetric growth, shape and composition of a growing tumor. Importantly, while we do present some of our results in two dimensions, the algorithm is readily applied to tumors growing in three-dimensional space, as illustrated in figure 2.

Our simulations have shown that in an arbitrarily shaped growth-permitting region, the original algorithm insists on imposing spherically symmetric tumor growth independent of the shape of the environment. On the other hand, the modified algorithm presented here allows the tumor to adapt its shape based on the constraints imposed by the confining region in which it grows and the obstacles to growth found within this region. This is comparable to what has been observed experimentally, where a tumor growing in a capillary tube develops as an ellipsoid. However, the same tumor grown in a gel that is not confined to a capillary tube develops as a sphere, highlighting the effects of physical confinement on the shape of a developing tumor [12]. Just as the shape of a tumor is altered by the confined environment in which it grows, the same can be said for the volumetric growth of the tumor. We have shown that there is a disagreement between the size of a tumor as a function of time when the original and modified algorithms are implemented. The discrepancies observed between a tumor growth algorithm that assumes spherically symmetric growth and one that makes no assumptions on the geometric form of a neoplasm highlights the importance of incorporating tumor–boundary interactions and environmental heterogeneity in any clinically relevant model of tumor growth.

The computational results presented above are illustrative in nature and describe some general scenarios in which the growing tumor encounters boundaries or obstacles of

somewhat idealized geometries. However, the latent power of the technique lies in the ability of the model to extend to ever more complex or multiply connected geometrical structures, such as cases where a large region of the cerebrovascular tree must be considered. One can also foresee an extension of the model to cases where the dynamics are more complex, for example a lung tumor near the individual moving ribs of the chest, or a spinal cord tumor subject to arbitrary if not continuous torsional movements of the neck and spine. Further extensions of the work might include cases where either pooling or circulation of an interstitial fluid (ISF) establishes either a physical (obstacle-like) or flow-field boundary condition (the equivalent of a fluid dynamical stationary state). An example of the former might be an edematous mass that grows jointly with the tumor, each influencing the size and shape of the other. For the other case, consider that the net flux of ISF in the brain parenchyma of small mammals is thought to be between 100 and 300 nl min⁻¹ per gram of tissue [32], which would imply that for an adult human brain of 1.4 kg, the net flux of ISF through the brain would be about 300 nl min⁻¹, i.e., 0.43 liters per day. This is a relatively fast flow compared with the time scale of brain tumor growth rates, thus implying the presence of a kind of moving background that might also modify predicted rates of tumor growth. To account for these more complex scenarios, the model must be generalized to not only examine how the host deforms the tumor, but also to analyze the reciprocal deformities induced in the host by the growing neoplasm. The addition of this feedback into the model is critical to quantitatively predicting tumor size, shape and spread.

The notion of incorporating computational models of tumor growth into the clinic complements the goal of individualizing tumor treatment strategies. The demand imposed on these algorithms would be very high. Limited information on the patient will be available, including tumor type (e.g., based on the pathology of biopsy samples), a genetic profile of the tumor (supplying, among other things, p53 status) and the location of the tumor within the body part or organ. Some examples of types information that may not necessarily be available as input to the computational model would include, e.g., for the case of gliomas, the intracranial pressure gradient within the tumor, the flow field of the interstitial fluid and the degree of blood–brain barrier disruption. However, in spite of incomplete physiological data on the tumor, a computer simulation should nevertheless be able to predict the size, shape and spread of the tumor at a fixed point in time, within the limits of accuracy that will be dictated by clinical standards of care. One important step in properly predicting these features is accounting for the location of the tumor within an organ, and how organ shape, heterogeneity and the placement of the tumor within the organ influence neoplastic progression.

In this paper, we have developed a set of automaton rules that are intended to move the field in that direction. However, any algorithm that can be used in the clinic must go far beyond predicting tumor size and shape. These algorithms must also predict the changes induced in the host by the growing tumor and the impact that multiple treatment strategies would have

on halting the progression of the tumor. With this goal in mind, the set of automaton rules proposed herein must be combined with more biologically detailed models of tumor growth. A first step in that direction would be implementing the new automaton rules in the previously developed hybrid cellular automaton model that examines the feedback that occurs between a neoplasm and the host microvasculature [8]. By adding further levels of complexity into the simple algorithm proposed here (such as a microscopic description of tissue structure and transport [33, 34]), the model can be built up step-by-step into a useful tool that can ultimately be of practical value to clinicians in predicting tumor growth patterns and guiding treatment strategies.

Acknowledgments

The work at the University of Virginia was supported in part by a grant from the Kopf Family Foundation, Inc.

Glossary

Neoplasm. A neoplasm is a synonym for a tumor.

Glioma. A collection of tumors arising from the glial cells or their precursors in the central nervous system.

Cellular automaton. A spatially and temporally discrete model that consists of a grid of cells, with each cell being in one of a number of predefined states. The state of a cell at a given point in time depends on the state of itself and its neighbors at the previous discrete time point. Transitions between states are determined by a set of local rules.

Growth-permitting environment. In our algorithm, this is the region of space in which the tumor can grow.

Voronoi cell. Given a set of points, the Voronoi cell is the cell that is formed about an arbitrary point in the set by finding the region of space closer to that point than any other point in the system [21].

Delaunay triangulation. Given a Voronoi graph (a set of Voronoi cells), the Delaunay graph is its dual that results from joining all pairs of sites that share a Voronoi face. If this graph consists of only simplices, the graph is called a Delaunay triangulation [21].

Quiescent. A cell is considered quiescent if it is in the G0 phase of the cell cycle and is not actively dividing.

Necrotic. A cell is considered necrotic if it has died due to injury or disease, such as abnormally low oxygen levels.

Edematous mass. A region of tissue that is swollen due to an excessive accumulation of fluid.

References

- [1] Bankhead A III and Heckendorn R B 2007 Using evolvable genetic cellular automata to model breast cancer *Genet. Programming Evolvable Mach.* **8** 381–93
- [2] Spencer S L, Gerety R A, Pienta K J and Forrest S 2006 Modeling somatic evolution in tumorigenesis *PLoS Comput. Biol.* **2** e108
- [3] Gatenby R A 1996 Application of competition theory to tumour growth: implications for tumour biology and treatment *Eur. J. Cancer A* **32** 722–26
- [4] Alarcón T, Byrne H M and Maini P K 2005 A multiple scale model for tumor growth *Multiscale Model. Simul.* **3** 440–75
- [5] Bellomo N and Preziosi L 2000 Modelling and mathematical problems related to tumor evolution and its interaction with the immune system *Math. Comput. Model.* **32** 413–52
- [6] de Pillis L G, Radunskaya A E and Wiseman C L 2005 A validated mathematical model of cell-mediated immune response to tumor growth *Cancer Res.* **65** 7950–8
- [7] Scalerandi M, Capogrosso Sansone B and Condat C A 2001 Diffusion with evolving sources and competing sinks: development of angiogenesis *Phys. Rev. E* **65** 011902
- [8] Gevertz J L and Torquato S 2006 Modeling the effects of vasculature evolution on early brain tumor growth *J. Theor. Biol.* **243** 517–31
- [9] Chen C Y, Byrne H M and King J R 2001 The influence of growth-induced stress from the surrounding medium on the development of multicell spheroids *J. Math. Biol.* **43** 191–220
- [10] Roose T, Netti P A, Munn L L, Boucher Y V and Jain R K 2003 Solid stress generated by spheroid growth estimated using a linear poroelasticity model *Microvasc. Res.* **66** 204–12
- [11] Kim Y, Stolarska M A and Othmer H G 2007 A hybrid model for tumor spheroid growth in vitro: I. Theoretical development and early results *Math. Models Methods Appl. Sci.* **17** (Suppl.) 1773–98
- [12] Helmlinger G, Netti P A, Lichtenbeld H C, Melder R J and Jain R K 1997 Solid stress inhibits the growth of multicellular tumor spheroids *Nat. Biotechnol.* **15** 778–83
- [13] Chen Z-J, Gillies G T, Broaddus W C, Prabhu S S, Fillmore H L, Mitchell R M, Corwin F D and Fatouros P P 2004 A realistic brain tissue phantom for intraparenchymal infusion studies *J. Neurosurg.* **101** 314–22
- [14] Deisboeck T S and Guiot C 2008 Surgical impact on brain tumor invasion: a physical perspective *Ann. Surg. Innov. Res.* **2** 1–6
- [15] Fillmore H L, Chasiotis I, Cho S W and Gillies G T 2003 Atomic force microscopy observations of tumour cell invadopodia: novel cellular nanomorphologies on collagen substrates *Nanotechnology* **14** 73–6
- [16] Chasiotis I, Fillmore H L and Gillies G T 2003 Atomic force microscopy measurement of cytostructural elements involved in the nanodynamics of tumour cell invasion *Nanotechnology* **14** 557–61
- [17] Geer C P and Grossman S A 1997 Interstitial fluid flow along white matter tracts: a potentially important mechanism for the dissemination of primary brain tumors *J. Neuro-Oncol.* **32** 193–201
- [18] Kansal A R, Torquato S, Harsh IV R G, Chiocca E A and Deisboeck T S 2000 Simulated brain tumor growth dynamics using a three-dimensional cellular automaton *J. Theor. Biol.* **203** 367–82
- [19] Kansal A R, Torquato S, Chiocca E A and Deisboeck T S 2000 Emergence of a subpopulation in a computational model of tumor growth *J. Theor. Biol.* **207** 431–41
- [20] Schmitz J E, Kansal A R and Torquato S 2002 Cellular automaton simulation of brain tumor treatment and resistance *J. Theor. Med.* **4** 223–39
- [21] Torquato S 2002 *Random Heterogeneous Materials: Microstructure and Macroscopic Properties* (New York: Springer)

- [22] Fortune S 1987 Sweep-line algorithms for Voronoi diagrams *Algorithmica* **2** 153–74
- [23] Donev A, Stillinger F H and Torquato S 2005 Neighbor list collision-driven molecular dynamics simulation for nonspherical particles: I. Algorithmic details *J. Comput. Phys.* **202** 737–64
- [24] Broaddus W C, Haar P J and Gillies G T 2004 *Encyclopedia of Biomaterials and Biomedical Engineering* (New York: Dekker)
- [25] Morrison P F, Laske D W, Bobo H, Oldfield E H and Dedrick R L 1994 High-flow microinfusion: tissue penetration and pharmacodynamics *Am. J. Phys.* **266** R292–305
- [26] Chen Z-J, Broaddus W C, Viswanathan R R, Raghavan R and Gillies G T 2002 Intraparenchymal drug delivery via positive pressure infusion: experimental and modeling studies of poroelasticity in brain phantom gels *IEEE Trans. Biomed. Eng.* **49** 85–96
- [27] Haar P J, Stewart J E, Gillies G T, Prabhu S S and Broaddus W C 2001 Quantitative three-dimensional analysis and diffusion modeling of oligonucleotide concentration after direct intraparenchymal brain infusion *IEEE Trans. Biomed. Eng.* **48** 560–9
- [28] Chiocca E A, Broaddus W C, Gillies G T, Visted T and Lamfers M L M 2004 Neurosurgical delivery of chemotherapeutics, targeted toxins, genetic and viral therapies in neuro-oncology *J. Neuro-Oncol.* **69** 101–17
- [29] Chen M Y, Chen Z-J, Gillies G T, Haar P J and Broaddus W C (ed) 2006 *Handbook of Brain Tumor Chemotherapy* (New York: Academic) chapter 20, pp 295–304
- [30] Sampson J H *et al* 2007 Clinical utility of a patient-specific algorithm for simulating intracerebral drug infusions *Neuro-Oncology* **9** 343–53
- [31] 2006 iPlan[®] Flow: more accurate planning for better outcomes. <http://www.brainlab.com/download/pdf/iPlanFlow.pdf>. Accessed 4/28/2008
- [32] Abbott N J 2004 Evidence for bulk flow of brain interstitial fluid: significance for physiology and pathology *Neurochem. Int.* **45** 545–52
- [33] Kim I C and Torquato S 1991 Effective conductivity of suspensions of spheres by Brownian motion simulation *J. Appl. Phys.* **69** 2280–9
- [34] Gevertz J L and Torquato S 2008 A novel three-phase model of brain tissue microstructure *PLoS Comput. Biol.* **4** e1000152